Proteinase-activated receptor 1 activation induces epithelial apoptosis and increases intestinal permeability

Alex C. Chin*†‡, Nathalie Vergnolle†§, Wallace K. MacNaughton†¶, John L. Wallace†§, Morley D. Hollenberg†§, and Andre G. Buret*†‖

†Mucosal Inflammation Research Group and Departments of *Biological Sciences, §Pharmacology and Therapeutics, and ¶Physiology and Biophysics, University of Calgary, Calgary, AB, Canada T2N 1N4

Edited by Pedro M. Cuatrecasas, University of California School of Medicine, La Jolla, CA, and approved July 1, 2003 (received for review March 13, 2003)

Proteinase-activated receptor 1 (PAR_1)-mediated inflammation remains poorly understood. Here we characterize previously unrecognized effects of PAR_1-induced apoptosis signaling, which contributes to epithelial barrier dysfunction. Incubation of epithelial cells with PAR_1 agonists induced apoptosis and increased epithelial permeability in a caspase-3-dependent manner. Similarly, studies *in vivo* demonstrated that intracolonic infusion with PAR_1 agonists increased colonic permeability in mice, and that this effect was abolished by pretreatment with a caspase-3 inhibitor. PAR_1 agonists induced tight junctional zonula-occludens 1 disruption and apoptotic nuclear condensation. Investigation into signaling pathways showed that these effects were dependent on caspase-3, tyrosine kinase, and myosin light chain kinase. Conversely, the Src kinase inhibitor PP1 augmented zonula-occludens 1 injury and nuclear condensation induced by PAR_1 agonists. These results support a role for proteinases and PARs in intestinal disease and provide new directions for possible therapeutic applications of PAR_1 antagonists.

Proteinase-activated receptors (PARs) are G protein-coupled signaling receptors that require the cleavage of their extracellular N terminus by proteinases such as thrombin, trypsin, and tryptase (1). The resulting exposed tethered ligand binds and activates the cleaved receptors. Synthetic peptides that correspond to the tethered ligands can also specifically activate PARs (2, 3).

The first PAR to be cloned, PAR_1, is activated by thrombin and has a central regulatory role in inflammation as it modulates platelet aggregation, vasodilation, and vasoconstriction, increased vascular permeability, granulocyte chemotaxis, and calcium-dependent chloride secretion in intestinal epithelial cells (1, 4, 5). Indeed, thrombin has been implicated in a number of inflammatory diseases, including inflammatory bowel disease (IBD) (6–8). The pathogenesis of IBD involves increased intestinal permeability (9). In addition, there is increased enterocyte apoptosis in biopsies obtained from ulcerative colitis patients (10). A link between apoptosis and changes in epithelial permeability has been highlighted by recent studies in which enterocyte apoptosis was induced by drugs, immune factors, or microbes (11–14). Although activation of PAR_2 by extracellular proteinases or selective PAR_2 agonists can increase intestinal permeability and bacterial translocation in mice (15), the impact of PAR_1 activation in this regard has yet to be determined. Because thrombin-mediated activation of PAR_1 can induce apoptosis in cultured neurons, astrocytes, as well as tumorigenic cell lines, and because epithelial apoptosis has been associated with increased epithelial permeability, we hypothesized that PAR_1-mediated effects on intestinal permeability may be linked to the activation of the apoptotic signaling pathway (16, 17).

In an attempt to test this hypothesis, the aims of the present study were: (*i*) to investigate whether PAR_1 agonists can alter epithelial permeability and whether this effect is attributable to enterocyte apoptosis, (*ii*) to determine whether PAR_1-induced apoptosis disrupts tight junctional zonula-occludens (ZO)-1 and to identify the signaling pathways implicated in this injury, and (*iii*) to assess whether PAR_1 activation can alter intestinal permeability *in vivo* and whether this effect is apoptosis-dependent.

Methods

***In Vitro* Cell Culture Model.** All *in vitro* experiments were done by using the nontumorigenic epithelial cell line, SCBN. SCBN was originally isolated from a human duodenal biopsy, grows into polarized confluent monolayers, possesses cytokeratins, mucin and sucrase-isomaltase antigens, mRNA for epidermal growth factor, interleukin-6, and vascular cell adhesion molecule-1, cytoskeletal proteins sensitive to microbes, calcium-dependent chloride secretion, and expresses PAR_1 (4, 18, 19). Cells were grown in DMEM (Sigma), supplemented with 5% heat-inactivated FBS, 100 μg/ml streptomycin, 100 units/ml penicillin, 0.08 mg/ml tylosin, and 200 mM L-glutamine (all from Sigma) as described (14). Cells were incubated at 37°C and 5% CO_2 in 96% humidity. Culture media was replenished every 2–3 days, and the cells were passaged by using 2× trypsin-EDTA (Sigma). Trypsinized cells (2.0×10^5 cells per ml) were added to Lab-Tek chamber slides (Nalge Nunc) (400 μl), to 12-well tissue culture-treated plates (Costar, Cambridge, MA) (500 μl), or to Transwell filter units (Costar) (500 μl) that contained a 1.13 cm^2 semipermeable filter membrane with 0.4-μm pores. Each Transwell filter unit was incubated in 12-well cluster plates (Costar). In all studies, SCBN cells were used between passages 23 and 27.

PAR_1 Agonists. The selective PAR_1 activating (Thr-Phe-Leu-Leu-Arg, TFLLR-NH_2) and inactive control (Arg-Leu-Leu-Phe-Thr, RLLFT-NH_2) peptides were prepared by solid-phase synthesis at the Peptide Synthesis Facility of the University of Calgary. The composition and purity of the peptides and the concentrations of stock solutions were verified by using HPLC and mass spectral and amino acid analysis. The PAR_1 agonist TFLLR-NH_2 has been found to be a selective activator of PAR_1, and human thrombin (Calbiochem) activates PAR_1 (20).

***In Vitro* Studies.** For assessment of apoptosis [Hoechst fluorescence staining 33258 (Molecular Probes) and ELISA] and characterization of tight junctional ZO-1 integrity, epithelial monolayers were used 5 days after passage, a time at which they

This paper was submitted directly (Track II) to the PNAS office.

Abbreviations: PAR, proteinase-activated receptor; IBD, inflammatory bowel disease; Z-DEVD-FMK, Z-Asp(OCH_3)-Glu(OCH_3)-Val-Asp(OCH_3)-FMK; MLCK, myosin light chain kinase; TFLLR, Thr-Phe-Leu-Leu-Arg; RLLFT, Arg-Leu-Leu-Phe-Thr; ZO, zonula-occludens.

‡Present address: Division of Gastrointestinal Pathology, Department of Pathology and Laboratory Medicine, Emory University School of Medicine, Atlanta, GA 30322.

‖To whom correspondence should be addressed. E-mail: aburet@ucalgary.ca.

www.pnas.org/cgi/doi/10.1073/pnas.1831452100

had reached confluence but not overgrowth. Permeability was measured in Transwells 7 days after seeding on epithelial monolayers that reached peak electrical resistance (>1,000 Ω/cm^2). Monolayers were pretreated for 1 h at 37°C and 5% CO_2, with either 0.8% DMSO vehicle, membrane-permeable 120 μM caspase-3 inhibitor II (Z-DEVD-FMK, Z-Asp(OCH_3)-Glu(OCH_3)-Val-Asp(OCH_3)-FMK; Calbiochem), which irreversibly inhibits apoptosis (21), 5 μM PP1 (Calbiochem), which blocks Src (22), 10 μM tyrphostin (A23/AG18; Calbiochem), which inhibits tyrosine kinases (23), or 40 μM ML-9 (Sigma), which blocks myosin light chain kinase (MLCK) (24). After pretreatment with DMSO or the selective inhibitors dissolved in DMSO, monolayers were coincubated with either 5% DMEM (control), 25 μM TFLLR-NH_2, which is known to activate PAR_1 signaling (25), 25 μM RLLFT-NH_2, or 5 units/ml (vol/vol) human thrombin, which is known to induce platelet aggregation. The proapoptotic topoisomerase-I inhibitor, camptothecin (2 μg/ml; Sigma), was used as a positive control.

Apoptosis. Enterocyte apoptosis was quantified 2 and 24 h after challenge by using a Cell Death Detection ELISA kit (Roche Diagnostics). This immunoassay specifically detects the histone region (H1, H2A, H2B, H3, and H4) of mono- and oligonucleosomes that are released during apoptosis. Plates were read (405 nm) at 5-min intervals by using a THERMOmax microplate reader (Molecular Devices). Apoptosis was measured in duplicate from 10^5 enterocytes from each group and expressed as absorbance ratios of the experimental cell lysates versus absorbances calculated from controls and arbitrarily set at 1.0 at 30 min development. The detection limit for this ELISA is 10^2 apoptotic cells.

***In Vitro* Permeability.** To confirm monolayer confluence, transepithelial resistance was measured with an electrovoltohmeter (EVOM; World Precision Instruments, Sarasota, FL) in 12 separate monolayers grown on Transwells (Costar) before the study. Each monolayer reached a peak resistance >1,000 Ω/cm^2 by day 7 (data not shown). Electrical resistance was not measured in subsequent studies to avoid any possible disruption of the epithelial barrier integrity before experimentation. Effects of PAR_1 agonists on barrier function were evaluated in the absence or in the presence of the caspase-3 inhibitor Z-DEVD-FMK in monolayers prepared as above. Permeability to a dextran probe (3,000 Da) was assessed as described (14). Briefly, 2 and 24 h after inoculation, the apical and basolateral compartments were washed gently two times with warmed (37°C) sterile bicarbonate buffered Ringer's solution (115 mM NaCl/50 mM $NaHCO_3$/2.8 mM KH_2PO_4/2.8 mM K_2HPO_4/1.2 mM $CaCl_2$/1.2 mM $MgCl_2$/10 mM glucose, pH 7.4). A nonabsorbable FITC-conjugated dextran probe (100 μM in Ringer's solution, 3,000 MW; Molecular Probes) was added to the apical compartment, and Ringer's solution was added to the basolateral compartment. After 3-h incubation (37°C, 5% CO_2, 96% humidity), relative fluorescent units of basolateral samples were calculated with a microplate fluorometer (Spectra Max Gemini, Molecular Devices). Values were expressed as % apical FITC–dextran $\times 10^{-3}$ per cm^2 per h that crossed the Transwell membrane (14).

ZO-1 and Hoechst. Monolayers grown in chamber slides (Nalge Nunc) for 5 days were used to determine the effects of PAR_1 agonists on tight junctional ZO-1 integrity and apoptotic chromatin condensation 2 and 24 h after challenge. To assess whether changes were caused by apoptosis, experiments characterized the effects of the caspase-3 inhibitor, Z-DEVD-FMK, on the tight junctional ZO-1 alterations induced by PAR_1 agonists. Further experiments characterized the effects of PP1, tyrphostin (A23/AG18), and ML-9 to determine the involvement of Src kinases, the tyrosine kinases, and MLCK, respectively. Monolayers were fixed with fresh 2% paraformaldehyde (Polysciences, Warrington, PA) in isotonic PBS (136.9 mM NaCl/2.7 mM KCl/4.4 mM Na_2HPO_4 $4H_2O$/1.5 mM KH_2PO_4, pH 7.4; 2 h, room temperature) and washed with PBS. Cells were permeabilized with 0.5% Triton X-100 (Sigma) (15 min, room temperature), nonspecific antibody binding was blocked by using FBS (undiluted, Sigma) (10 min, room temperature), and monolayers were incubated (37°C, 1 h, humid chamber) with affinity-purified polyclonal rabbit anti-ZO-1 (1:100 in PBS; Zymed Laboratories, San Francisco), and then with Cy3-conjugated sheep anti-rabbit IgG (1:100 in PBS, Sigma). Cells were costained with the nuclear-specific dye Hoechst (1 μM; Molecular Probes) (30 min, dark humid chamber), mounted with Aqua PolyMount (Polysciences), and visualized under a Leica DMR fluorescence microscope. Enterocytes (%) that exhibited tight junctional ZO-1 disruption and/or apoptotic nuclear condensation and fragmentation were calculated in blinded fashion from five randomly selected areas on each coded slide. Photomicrographs were taken on a Photometrics CoolSNAP digital camera (Roper Scientific, Tucson, AZ).

***In Vivo* Studies.** Male C57Bl6 mice (6 weeks old; Charles River Laboratories) were housed in a controlled environment (22°C, 40% humidity, 12:12 h photoperiods) and had free access to food and water. Care and experimental practices were conducted under the standards of the Canadian Council on Animal Care and approved by the Animal Care Committee of the University of Calgary.

After a 12-h fast, under light halothane anesthesia, a polyethylene catheter was inserted intrarectally to 3–4 cm from the anus. A single injection of TFLLR-NH_2 (200 μg per mouse) or RLLFT-NH_2 (200 μg per mouse) were administered into the distal colon through the catheter, in a volume of 100 μl. Three hours later and under deep anesthesia (60 mg/kg ketamine and 25 mg/kg xylazine), mice received an intracolonic infusion of 75 μl of ^{51}Cr-EDTA at 2×10^6 cpm/h for 3 h. Intestinal permeability was assessed by measuring the passage of ^{51}Cr-EDTA from the colonic lumen to the blood. Blood was collected by cardiac puncture and was then measured for counts by using a γ counter. In separate experiments, the effects of a caspase-3 inhibitor on TFLLR-NH_2-induced colonic permeability were assessed by treating the animals with an intracolonic injection of 1.2 mM Z-DEVD-FMK (Biomol, Plymouth Meeting, PA) or 0.1% DMSO vehicle (100 μl). One hour later, they received intracolonic TFLLR-NH_2 or RLLFT-NH_2 (200 μg in 100 μl). Intestinal permeability was measured as described above. Immunohistochemistry for caspase-3 (rabbit anti-active caspase-3, BD PharMingen) was performed on colonic tissues fixed in 10% buffered formalin.

Statistical Analysis. Results were expressed as means ± SEM and compared by one-way ANOVA, followed by Tukey's test for multiple comparison analysis where applicable. For the *in vivo* studies, results were expressed as means ± SEM, and significance was estimated by using the appropriate version of Student's *t* test. Statistical significance was established at $P < 0.05$.

Results

PAR_1 Agonists Induce Enterocyte Apoptosis. First, experiments assessed the effects of PAR_1 agonists on enterocyte apoptosis based on the production of apoptotic nucleosomes. After 2 or 24 h of incubation, either TFLLR-NH_2 or thrombin significantly increased the induction of apoptosis within monolayers (Fig. 1). In contrast, enterocyte apoptosis in monolayers exposed for 2 or 24 h to the control peptide RLLFT-NH_2 did not significantly differ from controls (Fig. 1).

PHYSIOLOGY

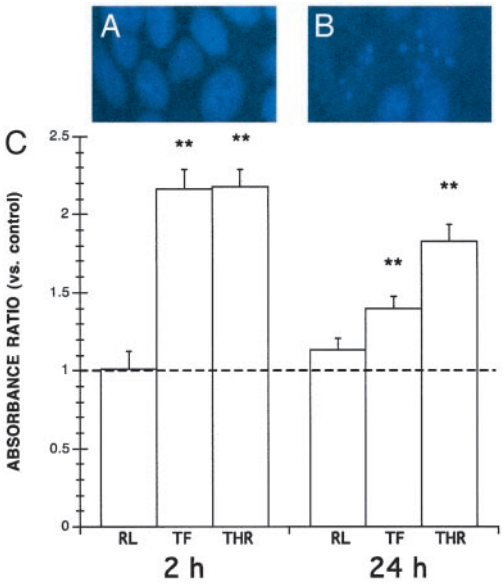

Fig. 1. PAR_1 agonists induce enterocyte apoptosis. Shown are representative Hoechst fluorescence micrographs of viable cells exhibiting uniform nuclear staining (*A*), and apoptotic cells exhibiting nuclear condensation (*B*). (*C*) Levels of apoptosis in epithelial monolayers incubated with 5% DMEM growth medium alone (−) or with 25 μM TFLLR-NH_2 (TF), 5 units/ml thrombin (THR), or 25 μM RLLFT-NH_2 (RL). Values at 30 min ELISA development were calculated as absorbance ratios versus control values arbitrarily set at 1.0 (−). Values are mean ± SEM; $n = 18$ per group; **, $P < 0.01$ compared with control.

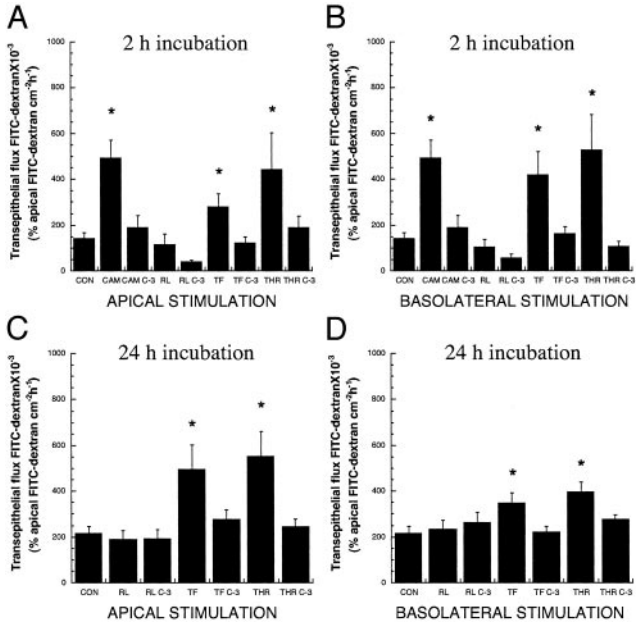

Fig. 2. PAR_1-induced enterocyte apoptosis increases epithelial permeability. Transepithelial fluxes of FITC-dextran 3000 across epithelial monolayers pretreated with or without caspase-3 inhibitor Z-DEVD-FMK (C-3) before incubation with either apical or basolateral 5% DMEM, 2 μg/ml camptothecin (CAM), 25 μM RLLFT-NH_2 (RL), 25 μM TFLLR-NH_2 (TF), or 5 units/ml thrombin (THR) for 2 h (*A* and *B*) or 24 h (*C* and *D*). Values are mean ± SEM; $n = 9$–16 per group; *, $P < 0.05$ compared with control.

PAR_1-Induced Apoptosis Increases Epithelial Permeability *in Vitro*. Next, experiments investigated whether induction of enterocyte apoptosis by PAR_1 activation contributes to epithelial injury by assessing the effects of PAR_1 agonists on transepithelial permeability, with or without pretreatment with a caspase-3 inhibitor. After 7 days of culture, the confluence of SCBN monolayers grown on Transwells was confirmed by low transepithelial FITC-dextran fluxes after 2 h (0.14 ± 0.02; $n = 16$) and 24 h incubation (0.22 ± 0.03; 24 h; $n = 16$) with vehicle alone (Fig. 2). In contrast, when compared with control values, in monolayers exposed to TFLLR-NH_2 or thrombin for 2 or 24 h, transepithelial fluxes were increased >2- to 3-fold when the PAR_1 agonists were added apically (Fig. 2 *A* and *C*) or when added basolaterally (Fig. 2 *B* and *D*), whereas the control peptide RLLFT-NH_2 failed to increase permeability. Pretreatment with Z-DEVD-FMK abolished the increase in transepithelial flux induced by TFLLR-NH_2, thrombin, and camptothecin, and maintained fluxes similar to controls. The increase in transepithelial fluxes induced by TFLLR-NH_2 and thrombin at both time points were near the levels induced by the proapoptotic compound camptothecin at 2 h (Fig. 2 *A* and *B*).

Activation of PAR_1 Increases Colonic Permeability. To assess the physiological significance of the *in vitro* studies, the next series of experiments investigated the effects of PAR_1 activation on intestinal permeability *in vivo*. For these experiments, the effects of the selective PAR_1 agonist TFLLR-NH_2 on colonic permeability were assessed in mice, with or without caspase-3 inhibitor pretreatment. After 3 h, mice intracolonically infused with TFLLR-NH_2, but not RLLFT-NH_2, had increased levels of ^{51}Cr-EDTA in the blood (Fig. 3*A*). Conversely, pretreatment with the selective caspase-3 inhibitor significantly inhibited the increase in ^{51}Cr-EDTA and maintained levels similar to controls (Fig. 3*B*). Immunohistochemistry revealed significantly higher levels of caspase-3 activation in colonic tissues exposed to TFLLR-NH_2 than in those exposed to RLLFT-NH_2 (Fig. 7, which is published as supporting information on the PNAS web site, www.pnas.org).

PAR_1-Induced Apoptosis Disrupts Tight Junctional ZO-1 via Caspase-3, Tyrosine Kinases, and MLCK. In an attempt to uncover PAR_1 signaling pathways leading to epithelial injury, experiments assessed the effects of selective kinase inhibitors on tight junctional ZO-1 and epithelial apoptosis on PAR_1 activation. After 2 h of incubation, control monolayers exhibited continuous pericellular organization of ZO-1 in conjunction with uniform fluorescent nuclear staining characteristic of viable cells (Fig. 4*A*). In contrast, monolayers incubated with TFLLR-NH_2 or thrombin exhibited focal disruptions, punctate relocalization, and cytosolic diffusion of ZO-1, as well as an increase in the incidence of chromatin condensation and nuclear fragmentation (Fig. 4 *B* and *C*). These abnormalities were abolished by pre-

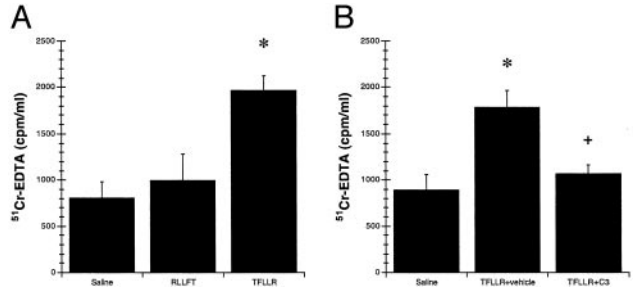

Fig. 3. Induction of apoptosis by activation of PAR_1 increases colonic permeability. Blood levels of ^{51}Cr-EDTA after intracolonic administration with saline vehicle, 200 μg of TFLLR-NH_2, or 200 μg of RLLFT-NH_2 (*A*) or with saline vehicle, 200 μg of TFLLR-NH_2, or with 200 μg of TFLLR-NH_2 after pretreatment with caspase-3 inhibitor Z-DEVD-FMK (*B*). Values are mean ± SEM; $n = 8$ per group; *, $P < 0.05$ compared with control peptide; +, $P < 0.05$ compared with TFLLR-NH_2 treatment.

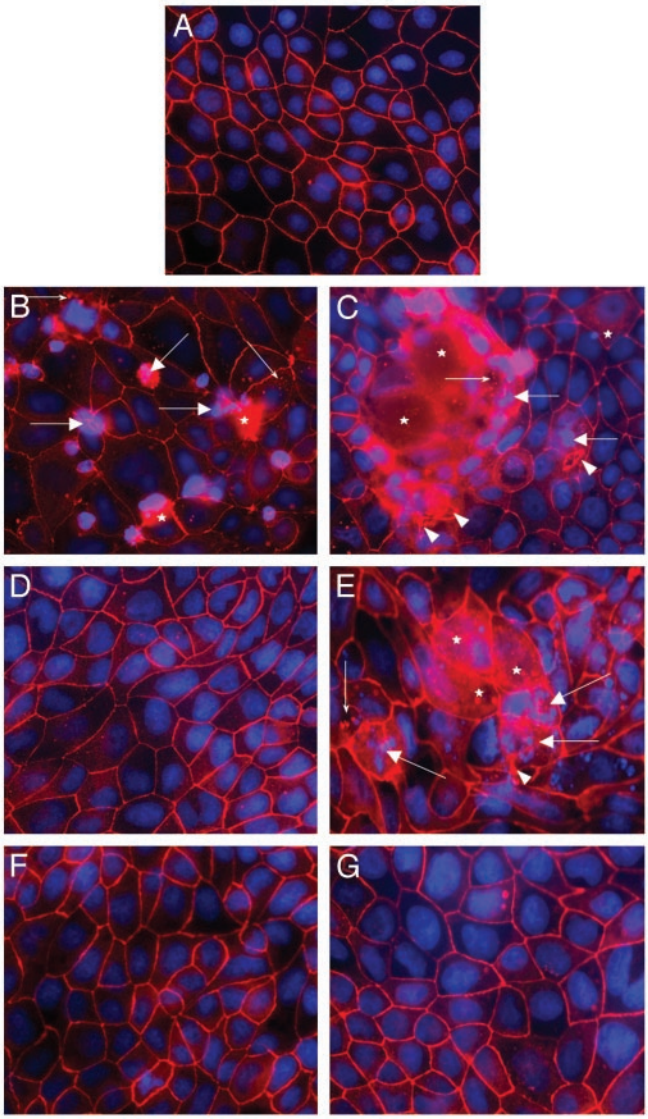

Fig. 4. PAR_1-induced enterocyte apoptosis disrupts tight junctional ZO-1 in a caspase-3-, tyrosine kinase-, and MLCK-dependent manner. Shown are representative micrographs illustrating ZO-1 and nuclear integrity in epithelial monolayers after 2 h. Preparations were coincubated with 5% DMEM growth medium (*A*), 25 μM TFLLR-NH_2 (*B*), 5 units/ml thrombin (*C*), caspase-3 inhibitor Z-DEVD-FMK and 25 μM TFLLR-NH_2 (*D*), Src inhibitor PP1 and 25 μM TFLLR-NH_2 (*E*), tyrosine kinase inhibitor tyrphostin and 25 μM TFLLR-NH_2 (*F*), or MLCK inhibitor ML-9 and 25 μM TFLLR-NH_2 (*G*). Cellular changes include focal disruption of ZO-1 along the pericellular junctions (arrowhead), punctate ZO-1 redistribution (small arrows), diffuse intracellular ZO-1 relocalization (asterisk), and apoptotic nuclear condensation (large arrows). All micrographs were obtained at a magnification of ×400.

treatment with the caspase-3 inhibitor Z-DEVD-FMK before incubation with TFLLR-NH_2 (Fig. 4*D*) or thrombin (data not shown). Conversely, pretreatment with the Src-targeted inhibitor PP1 appeared to intensify the tight junctional ZO-1 injury and the incidence of apoptotic nuclear morphology induced by TFLLR-NH_2 (Fig. 4*E*) or thrombin (data not shown). However, pretreatment with both the nonselective tyrosine kinase inhibitor tyrphostin A23/AG18 or the MLCK inhibitor ML-9 prevented the ZO-1 and apoptotic changes induced by 25 μM TFLLR-NH_2 (Fig. 4*F*) or thrombin (data not shown). Similar results were observed after 24 h (data not shown). Except for the Src inhibitor PP1 which alone increased ZO-1 and nuclear

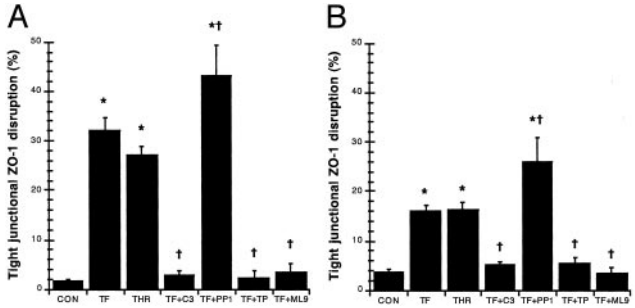

Fig. 5. PAR_1 agonists disrupt tight junctional ZO-1 via caspase-3, tyrosine kinases, and MLCK. Quantification of ZO-1 disruption in monolayers incubated with 5% DMEM growth medium (CON), 25 μM TFLLR-NH_2 (TF), thrombin (THR), caspase-3 inhibitor Z-DEVD-FMK and 25 μM TFLLR-NH_2 (TF+C3), Src inhibitor PP1 and 25 μM TFLLR-NH_2 (TF+PP1), tyrosine kinase inhibitor tyrphostin and 25 μM TFLLR-NH_2 (TF+TP), or MLCK inhibitor ML-9 and 25 μM TFLLR-NH_2 (TF+ML9) for 2 h (*A*) or 24 h (*B*). Values are mean ± SEM; $n = 8$ per group; *, $P < 0.05$ compared with control; †, $P < 0.05$ compared with TFLLR-NH_2-treated monolayers.

abnormalities, incubation with the other inhibitors alone did not affect ZO-1 integrity and apoptosis.

Further quantification under fluorescence microscopy confirmed that incubation with TFLLR-NH_2 or thrombin (data not shown) increased ZO-1 disruption by close to 30-fold when compared with controls at 2 and 24 h, respectively (Fig. 5). Pretreatment with Z-DEVD-FMK, tyrphostin, and ML-9 prevented the ZO-1 alterations induced by PAR_1 agonists (thrombin data not shown) and maintained levels of controls at both 2 and 24 h (Fig. 5). However, pretreatment with PP1 further exacerbated the injury induced by PAR_1 activation (thrombin data not shown) by 40- and 25-fold when compared with controls at 2 and 24 h, respectively (Fig. 5). When compared with controls, the inhibitors alone did not affect ZO-1 organization, except for PP1 which increased ZO-1 disruption at 2 and 24 h (data not shown).

Apoptosis induced by PAR_1 activation was confirmed by quantification using Hoechst nuclear staining (Fig. 6). Monolayers incubated with TFLLR-NH_2 or thrombin (data not shown) increased the incidence of nuclear condensation by 10-fold and 4-fold when compared with controls at 2 and 24 h, respectively (Fig. 6). Pretreatment with Z-DEVD-FMK, tyrphostin, and ML-9 prevented the induction of apoptotic nuclear

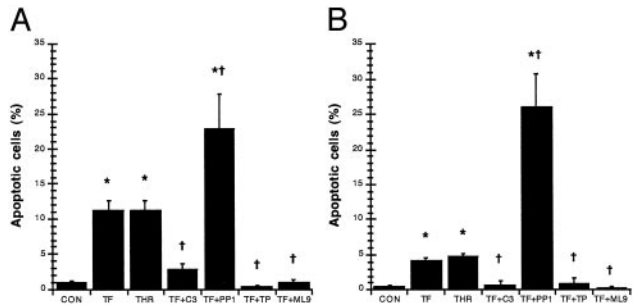

Fig. 6. PAR_1 agonists induce enterocyte apoptosis in a caspase-3-, tyrosine kinase-, and MLCK-dependent fashion. Quantification of apoptotic nuclear condensation in monolayers incubated with 5% DMEM growth medium (CON), 25 μM TFLLR-NH_2 (TF), thrombin (THR), caspase-3 inhibitor Z-DEVD-FMK and 25 μM TFLLR-NH_2 (TF+C3), Src inhibitor PP1 and 25 μM TFLLR-NH_2 (TF+PP1), tyrosine kinase inhibitor tyrphostin and 25 μM TFLLR-NH_2 (TF+TP), or MLCK inhibitor ML-9 and 25 μM TFLLR-NH_2 (TF+ML9) for 2 h (*A*) or 24 h (*B*) is shown. Values are mean ± SEM; $n = 8$ per group; *, $P < 0.05$ compared with control; †, $P < 0.05$ compared with TFLLR-NH_2-treated monolayers.

changes induced by PAR_1 agonists (thrombin data not shown) and maintained levels similar to controls at both 2 and 24 h (Fig. 6). However, pretreatment with PP1 further increased the nuclear condensation induced by PAR_1 activation (thrombin data not shown) by 20- and 25-fold when compared with controls at 2 and 24 h, respectively (Fig. 6). The inhibitors alone did not significantly affect nuclear structure compared with controls, except for PP1 which increased nuclear condensation at 2 and 24 h (data not shown).

Discussion

Findings from this study draw a link between PAR_1 induction of the apoptotic signaling pathway and the ability of thrombin acting via PAR_1 to regulate permeability of intestinal epithelial monolayers. Furthermore, this link can be extended to the ability of PAR_1 activation to increase intestinal permeability *in vivo*. Pretreatment with inhibitors of caspase-3 (Z-DEVD-FMK), tyrosine kinase (tyrphostin), or MLCK (ML-9) abolished the increase in tight junctional ZO-1 disruption and apoptotic nuclear condensation induced by PAR_1 agonists. Conversely, pretreatment with PP1 a Src-family-targeted inhibitor had the opposite effects and increased ZO-1 disruption and apoptosis. Furthermore, PAR_1 activation *in vivo* increased colonic permeability and this effect was prevented by caspase-3 inhibition. Together, the results show that PAR_1 signaling events leading to heightened apoptosis and subsequent loss of barrier function require caspase-3, a non-Src tyrosine kinase, and MLCK. This novel biological cascade may be an important factor of the pathogenesis of mucosal diseases, which involve host or microbial proteinases that may activate PAR_1.

Serine proteinases such as trypsin, tryptase, and thrombin have been shown to activate PARs, which are known to be involved in inflammatory processes (1, 15, 26–31). Thrombin, which activates PAR_1, has been implicated in the pathogenesis of IBD (6–8). Furthermore, recent studies have shown that thrombin induces apoptosis in cultured neurons, astrocytes, and tumorigenic cell lines by activated PAR_1 (16, 17). Findings from this study now show that apoptosis can be induced in intestinal epithelial systems via activation of PAR_1 by a specific agonist (TFLLR-NH_2). The proapoptotic effects of PAR_1 activation may explain the increased incidence of apoptotic cells during IBD (10) and may play a role in other disease states where high levels of thrombin are found. Further studies with specific PAR_1 antagonists, which as yet are not readily available, are warranted to confirm the proapoptotic effects of thrombin via PAR_1 activation in the induction of epithelial injury.

The intestinal epithelium acts both as a physical barrier by protecting the host from environmental pathogens, and as a selective barrier by allowing for exchanges of ions, small molecules and macromolecules (32). A compromised epithelium reflects the causes and/or consequences of various intestinal diseases including IBD, celiac disease, and bacterial enteritis (33). Although the physiological elimination of senescent enterocytes via apoptosis does not compromise epithelial barrier function (34), previous studies have shown that epithelial apoptosis enhanced by chemical (11), immune (12, 13), or microbial factors (14) does increase permeability. Similar to these observations, findings from this study show that PAR_1 agonists can increase epithelial permeability and that this effect can be abolished by inhibition of caspase-3. Perhaps more importantly, these findings further confirm the role of apoptosis in regulating epithelial permeability, and illustrate that the increase in epithelial permeability can occur with either apical or basolateral stimulation.

Epithelial tight junctional complexes are composed of proteins that belong to the ZO, claudin, occludin, and cingulin families (35). ZO-1 is a 220-kDa peripheral membrane protein that interacts with another tight junctional protein occludin at its N terminus and with cytoskeletal F-actin at its C terminus (35). Therefore, ZO-1 is ideally suited to regulate paracellular permeability by interacting with both the cytoskeleton and the tight junctional proteins. In an attempt to elucidate further the signaling pathway for PAR_1 activation in the present system, proteins that are involved in apoptosis (caspase-3), PAR_1 signaling (Src and other tyrosine kinases), and epithelial permeability (MLCK) were examined. Results from this study indicate that the effects of PAR_1 on apoptosis and permeability are dependent on caspase-3, non-Src family tyrosine kinases, and MLCK.

Cytoskeletal proteins such as actin, α-fodrin, and keratin, as well as adherens junctional components such as β-catenin and plakoglobin are cleaved by caspases, and this cleavage is responsible for the structural disintegration and membrane blebbing observed in apoptotic cells, and ultimately lead to detachment of cells from the substratum (36). Induction of apoptosis in colonic T84 monolayers by FasL is associated with disturbances in tight junctional proteins ZO-1, and desmoplakins 1 and 2 (13). Similarly, caspase-3 is required to cause epithelial permeability and tight junctional ZO-1 disruption in monolayers exposed to the intestinal protozoan pathogen *Giardia lamblia* (14). The present results now demonstrate that caspase-3-dependent alteration of tight junctional ZO-1 can be induced by activation of PAR_1.

The PAR_1 signaling mechanisms have been studied in some depth (37). PAR_1 couples to a variety of G proteins (Gq, Gi, G12, and G13) and can trigger signal pathways in common with those stimulated by the epidermal growth factor (EGF) receptor involving the activation of mitogen-activated protein (MAP) kinase, phosphotidylinositol kinase-3, protein kinase C, and possibly cellular Src (5, 38). In our attempt to characterize further the signaling mechanisms of PAR_1-induced apoptosis and ZO-1 disruption, we found that tyrosine kinases, apart from Src, may play an important role. The intriguing effects of the Src family-targeted inhibitor PP1 are highlighted further by studies assessing the role of Src-family kinases in apoptosis. One study has shown that the Src kinases Fyn and Lck are needed for Fas-mediated apoptosis in Jurkat cells (39). Conversely, an earlier study also using Jurkat cells has shown that inhibition of both Fyn and Lck augmented the apoptotic response (40), and yet another study showed that cleavage of Fyn and Lck occurs during apoptosis (41). Furthermore, inhibition of cytoproliferative v-Src has been shown to induce apoptosis (42), and a previous report has suggested that thrombin-induced apoptosis depends on tyrosine kinase (type unspecified) and overstimulation of RhoA (16). Moreover, tyrosine phosphorylation has been found to occur in apoptosis (43). During physiological conditions, Rho plays an important role in cytoskeletal organization, cell cycle progression, and apoptotic cellular rounding (44–46). Downstream from Rho, the ROCK serine/threonine kinase isoenzymes are involved in actin cytoskeletal rearrangement, tight junction function/assembly, and are major regulators of cellular contractility via MLCK (47, 48). Constitutively active cleavage products of ROCK I by caspases lead to increased phosphorylation of MLC and ultimately to the formation of apoptotic membrane blebbing and chromatin condensation (49–52). Consistent with these observations, and with the recent finding that MLCK regulates the opening of enterocyte tight junctional structures induced by *Giardia* (53), results from this study show that inhibition of MLCK by ML-9 inhibits both PAR_1-induced tight junctional ZO-1 disruption and apoptotic nuclear condensation. The implication of ROCK in PAR_1 signaling warrants further study.

In summary, the present report implicates caspase-3, non-Src family tyrosine kinases, and MLCK, in the induction of

tight junctional ZO-1 disruption and apoptosis caused by PAR_1 activation. The findings also demonstrate that the induction of apoptosis by PAR_1 activation is associated with increases in intestinal permeability *in vivo*. This novel biological pathway may be implicated in the pathogenesis of a number of disorders affecting mucosal surfaces, including IBD, asthma, and infectious diseases associated with the release of microbial proteinases. The therapeutic potential of PAR_1 antagonists in the setting of inflammatory disorders that affect intestinal or pulmonary epithelial permeability warrants further investigation.

We thank K. Chapman and M. Saifeddine for technical assistance. This work was supported by grants from the Natural Sciences and Engineering Research Council of Canada (to A.G.B.), the Alberta Heritage Foundation for Medical Research (to A.G.B., W.K.M., and J.L.W.), the Crohn's and Colitis Foundation of Canada (to A.G.B.), the Canadian Institutes of Health Research (to N.V., W.K.M., J.L.W., and M.D.H.), NicOx S.A. (to N.V.), and the Canadian Association of Gastroenterology (to N.V.).

1. Dery, O., Corvera, C. U., Steinhoff, M. & Bunnett, N. W. (1998) *Am. J. Physiol.* **274,** C1429–C1452.
2. Coughlin, S. R. (2000) *Nature* **407,** 258–264.
3. Hollenberg, M. D. & Compton, S. J. (2002) *Pharmacol. Rev.* **54,** 203–217.
4. Buresi, M. C., Schleihauf, E., Vergnolle, N., Buret, A., Wallace, J. L., Hollenberg, M. D. & MacNaughton, W. K. (2001) *Am. J. Physiol.* **281,** G323–G332.
5. Buresi, M. C., Buret, A. G., Hollenberg, M. D. & MacNaughton, W. K. (2002) *FASEB J.* **16,** 1515–1525.
6. Thompson, N. P., Wakefield, A. J. & Pounder, R. E. (1995) *Gastroenterology* **108,** 1011–1015.
7. Ghosh, S., Mackie, M. J., McVerry, B. A., Galloway, M., Ellis, A. & McKay, J. (1983) *Acta Haematol.* **70,** 50–53.
8. Wakefield, A. J., Sawyerr, A. M., Dhillon, A. P., Pittilo, R. M., Rowles, P. M., Lewis, A. A. & Pounder, R. E. (1989) *Lancet* **2,** 1057–1062.
9. Hollander, D., Vadheim, C. M., Brettholz, E., Petersen, G. M., Delahunty, T. & Rotter, J. I. (1986) *Ann. Intern. Med.* **105,** 883–885.
10. Strater, J., Wellisch, I., Riedl, S., Walczak, H., Koretz, K., Tandara, A., Krammer, P. H. & Moller, P. (1997) *Gastroenterology* **113,** 160–167.
11. Sun, Z., Wang, X., Wallen, R., Deng, X., Du, X., Hallberg, E. & Andersson, R. (1998) *Scand. J. Gastroenterol.* **33,** 415–422.
12. Gitter, A. H., Bendfeldt, K., Schulzke, J. D. & Fromm, M. (2000) *FASEB J.* **14,** 1749–1753.
13. Abreu, M. T., Palladino, A. A., Arnold, E. T., Kwon, R. S. & McRoberts, J. A. (2000) *Gastroenterology* **119,** 1524–1536.
14. Chin, A. C., Teoh, D. A., Scott, K. G., Meddings, J. B., MacNaughton, W. K. & Buret, A. G. (2002) *Infect. Immun.* **70,** 3673–3680.
15. Cenac, N., Coelho, A. M., Nguyen, C., Compton, S., Andrade-Gordon, P., MacNaughton, W. K., Wallace, J. L., Hollenberg, M. D., Bunnett, N. W., Garcia-Villar, R., *et al.* (2002) *Am. J. Pathol.* **161,** 1903–1915.
16. Donovan, F. M., Pike, C. J., Cotman, C. W. & Cunningham, D. D. (1997) *J. Neurosci.* **17,** 5316–5326.
17. Zain, J., Huang, Y. Q., Feng, X., Nierodzik, M. L., Li, J. J. & Karpatkin, S. (2000) *Blood* **95,** 3133–3138.
18. Pang, G., Buret, A., O'Loughlin, E., Smith, A., Batey, R. & Clancy, R. (1996) *Gastroenterology* **111,** 8–18.
19. Teoh, D. A., Kamieniecki, D., Pang, G. & Buret, A. G. (2000) *J. Parasitol.* **86,** 800–806.
20. Hollenberg, M. D., Saifeddine, M., al-Ani, B. & Kawabata, A. (1997) *Can. J. Physiol. Pharmacol.* **75,** 832–841.
21. Nicholson, D. W., Ali, A., Thornberry, N. A., Vaillancourt, J. P., Ding, C. K., Gallant, M., Gareau, Y., Griffin, P. R., Labelle, M., Lazebnik, Y. A., *et al.* (1995) *Nature* **376,** 37–43.
22. Hanke, J. H., Gardner, J. P., Dow, R. L., Changelian, P. S., Brissette, W. H., Weringer, E. J., Pollok, B. A. & Connelly, P. A. (1996) *J. Biol. Chem.* **271,** 695–701.
23. Levitzki, A. & Gilon, C. (1991) *Trends Pharmacol. Sci.* **12,** 171–174.
24. Turner, J. R., Rill, B. K., Carlson, S. L., Carnes, D., Kerner, R., Mrsny, R. J. & Madara, J. L. (1997) *Am. J. Physiol.* **273,** C1378–C1385.
25. Kawabata, A., Saifeddine, M., Al-Ani, B., Leblond, L. & Hollenberg, M. D. (1999) *J. Pharmacol. Exp. Ther.* **288,** 358–370.
26. Vergnolle, N., Hollenberg, M. D., Sharkey, K. A. & Wallace, J. L. (1999) *Br. J. Pharmacol.* **127,** 1083–1090.
27. Vergnolle, N. (1999) *J. Immunol.* **163,** 5064–5069.
28. Steinhoff, M., Vergnolle, N., Young, S. H., Tognetto, M., Amadesi, S., Ennes, H. S., Trevisani, M., Hollenberg, M. D., Wallace, J. L., Caughey, G. H., *et al.* (2000) *Nat. Med.* **6,** 151–158.
29. Vergnolle, N., Wallace, J. L., Bunnett, N. W. & Hollenberg, M. D. (2001) *Trends Pharmacol. Sci.* **22,** 146–152.
30. de Garavilla, L., Vergnolle, N., Young, S. H., Ennes, H., Steinhoff, M., Ossovskaya, V. S., D'Andrea, M. R., Mayer, E. A., Wallace, J. L., Hollenberg, M. D., *et al.* (2001) *Br. J. Pharmacol.* **133,** 975–987.
31. Vergnolle, N., Bunnett, N. W., Sharkey, K. A., Brussee, V., Compton, S. J., Grady, E. F., Cirino, G., Gerard, N., Basbaum, A. I., Andrade-Gordon, P., *et al.* (2001) *Nat. Med.* **7,** 821–826.
32. Kraehenbuhl, J. P., Pringault, E. & Neutra, M. R. (1997) *Aliment. Pharmacol. Ther.* **11,** Suppl. 3, 3–8; and discussion, 8–9.
33. Bjarnason, I., MacPherson, A. & Hollander, D. (1995) *Gastroenterology* **108,** 1566–1581.
34. Madara, J. L. (1990) *J. Membr. Biol.* **116,** 177–184.
35. Anderson, J. M. & Van Itallie, C. M. (1995) *Am. J. Physiol.* **269,** G467–G475.
36. Nicholson, D. W. (1999) *Cell Death Differ.* **6,** 1028–1042.
37. Macfarlane, S. R., Seatter, M. J., Kanke, T., Hunter, G. D. & Plevin, R. (2001) *Pharmacol. Rev.* **53,** 245–282.
38. Zheng, X. L., Renaux, B. & Hollenberg, M. D. (1998) *J. Pharmacol. Exp. Ther.* **285,** 325–334.
39. Schlottmann, K. E., Gulbins, E., Lau, S. M. & Coggeshall, K. M. (1996) *J. Leukoc. Biol.* **60,** 546–554.
40. Schraven, B. & Peter, M. E. (1995) *FEBS Lett.* **368,** 491–494.
41. Luciano, F., Ricci, J. E. & Auberger, P. (2001) *Oncogene* **20,** 4935–4941.
42. Johnson, D., Agochiya, M., Samejima, K., Earnshaw, W., Frame, M. & Wyke, J. (2000) *Cell Death Differ.* **7,** 685–696.
43. Rozengurt, E. & Rodriguez-Fernandez, J. L. (1997) *Essays Biochem.* **32,** 73–86.
44. Hall, A. (1998) *Science* **279,** 509–514.
45. Nusrat, A., von Eichel-Streiber, C., Turner, J. R., Verkade, P., Madara, J. L. & Parkos, C. A. (2001) *Infect. Immun.* **69,** 1329–1336.
46. Fiorentini, C., Fabbri, A., Falzano, L., Fattorossi, A., Matarrese, P., Rivabene, R. & Donelli, G. (1998) *Infect. Immun.* **66,** 2660–2665.
47. Amano, M., Fukata, Y. & Kaibuchi, K. (2000) *Exp. Cell. Res.* **261,** 44–51.
48. Walsh, S. V., Hopkins, A. M., Chen, J., Narumiya, S., Parkos, C. A. & Nusrat, A. (2001) *Gastroenterology* **121,** 566–579.
49. Sebbagh, M., Renvoize, C., Hamelin, J., Riche, N., Bertoglio, J. & Breard, J. (2001) *Nat. Cell Biol.* **3,** 346–352.
50. Coleman, M. L., Sahai, E. A., Yeo, M., Bosch, M., Dewar, A. & Olson, M. F. (2001) *Nat. Cell Biol.* **3,** 339–345.
51. Song, Y., Hoang, B. Q. & Chang, D. D. (2002) *Exp. Cell Res.* **278,** 45–52.
52. Mills, J. C., Stone, N. L., Erhardt, J. & Pittman, R. N. (1998) *J. Cell Biol.* **140,** 627–636.
53. Scott, K. G., Meddings, J. B., Kirk, D. R., Lees-Miller, S. P. & Buret, A. G. (2002) *Gastroenterology* **123,** 1179–1190.